Laboratory simulation of longitudinally cracked teeth using the step-stress cyclic loading method

F. Lin[1,2] (iD), R. Ordinola-Zapata[3] (iD), H. Xu[4] (iD), Y.C. Heo[2] & A. Fok[2] (iD)

[1]Department of Cariology and Endodontology, Peking University School and Hospital of Stomatology, Beijing, China; [2]Minnesota Dental Research Center for Biomaterials and Biomechanics, School of Dentistry, University of Minnesota, Minneapolis; [3]Division of Endodontics, Department of Restorative Sciences, School of Dentistry, University of Minnesota, Minneapolis, USA; and [4]Department of Stomatology, Affiliated Hospital of Qingdao University, Qingdao, China

Abstract

Lin F, Ordinola-Zapata R, Xu H, Heo YC, Fok A. Laboratory simulation of longitudinally cracked teeth using the step-stress cyclic loading method. *International Endodontic Journal*, **54**, 1638–1646, 2021.

Aim To simulate in a laboratory setting longitudinal cracking in root filled premolar teeth, using cyclic mechanical fatigue.

Methodology Mesial-occlusal-distal (MOD) cavities were prepared in twenty root filled, single-rooted, mandibular premolars restored with fibre posts and resin composites. The samples were randomly divided into two groups based on the loading approaches: static loading with a crosshead speed of 0.5 mm/min and step-stress cyclic loading (1 Hz) with increasing amplitude. The loads and numbers of cycles to failure were recorded. Micro-CT was also used to identify the fracture modes. Statistical analysis was performed using Student's t-test. The level of significance was set at 0.05.

Results The mean fracture loads for the static loading and cyclic loading groups were 769 ± 171 N and 720 ± 92 N, respectively. There was no significant difference between the two groups ($P > 0.05$). The proportions of longitudinal, cuspal and mixed-mode fractures under cyclic loading were 50%, 20% and 30%, respectively. Longitudinal fractures occurred with larger numbers of cycles and higher average loads per cycle compared with the other fractures. Static loading produced only cuspal fractures.

Conclusions Longitudinally cracked premolar teeth with root fillings were successfully produced using the step-stress cyclic loading method. This provides a more clinically representative methodology for studying cracked teeth in a laboratory setting.

Keywords: cracked tooth, cyclic loading, static loading, longitudinal fracture.

Received 5 August 2020; accepted 9 April 2021

Introduction

The cracked tooth, as one of the five categories of longitudinal tooth fractures, is defined by the American Association of Endodontists (AAE) as an incomplete vertical fracture initiated from the crown, extending subgingivally and usually directed mesiodistally (Rivera & Walton 2008). This injury can be caused by bruxism, trauma or excessive tooth destruction (Rivera & Walton 2007, 2008, Berman & Kuttler 2010,

Sim *et al.* 2016). Compared to cuspal fractures, the crack in a cracked tooth propagates longitudinally or even apically towards the root, resulting eventually in a split tooth (Rivera & Walton 2008).

Tooth cracking can occur in both teeth with vital pulps and root filled teeth (Seo *et al.* 2012). In the latter case, longitudinal cracks may appear on the proximal wall, cavity floor or pulp chamber floor. Since they are covered by dental restorations, these cracks are difficult to detect or visualize clinically (Rivera &

Correspondence: Alex Fok, 16-212 Moos Health Science Tower, 515 Delaware Street S.E., 55455, Minneapolis, MN, USA (e-mail: alexfok@umn.edu).

Walton 2007). This makes their early diagnosis and management challenging. Thus, the prognosis of root filled teeth with such longitudinal cracks is uncertain. Pain on chewing or even splitting of the tooth may occur if cracking is advanced or has affected the periodontium (Rivera & Walton 2007, Berman & Kuttler 2010). Hence, studying the cracked tooth is critical for investigating its mechanisms, propagation, diagnosis, treatment modalities and prognosis.

To date, studies on cracked teeth have focused on influencing factors (Tan *et al.* 2006, Sim *et al.* 2016, Wu *et al.* 2019), diagnosis (Sapra *et al.* 2020), treatment modalities (Kang *et al.* 2016, Alkhalifah *et al.* 2017) and prognosis (Tan *et al.* 2006, Berman & Kuttler 2010), most of which are clinical studies. Laboratory studies on this topic are limited due to the difficulty of acquiring extracted cracked teeth for investigation. Also, attempts to produce cracked teeth in a laboratory setting have provided inconsistent results. A common method to induce cracking in the laboratory is by thermal shocks; however, it is hard to control the orientation of the cracks using this method (Wang *et al.* 2017, Yuan *et al.* 2020).

Alternatively, a static load has been used in many laboratory studies to produce cracks in teeth (Krishan *et al.* 2014, Plotino *et al.* 2017, Corsentino *et al.* 2018, Özyürek *et al.* 2018). It is usually applied by lowering a load tip on to the sample under a certain crosshead speed until it fractures (Karzoun *et al.* 2015, Xiong *et al.* 2015). The fracture load thus obtained is usually very high. In some studies, the reported load necessary to fracture a tooth could be up to 1700-2500 N (Krishan *et al.* 2014, Corsentino *et al.* 2018, Özyürek *et al.* 2018), which is much higher than the normal chewing force (60-250 N) or even the maximum occlusal force during bruxing (~800 N) (Kelly 1997, Nishigawa *et al.* 2001). Moreover, the type of fracture induced by static loading is more likely to be cuspal fracture (Franco *et al.* 2014, Karzoun *et al.* 2015, Plotino *et al.* 2017, Özyürek *et al.* 2018) rather than longitudinal fracture. No studies have successfully reproduced the longitudinal fractures found in cracked teeth under static loading.

Cyclic loading, as a different mode of loading, is often used to approximate oral physiological mastication, which is thought to be an important aetiology for longitudinally cracked teeth (Rivera & Walton 2007, Banerji *et al.* 2010). However, it has been rarely used for fracture testing due to its long duration (Li *et al.* 2015). With a load amplitude and frequency representative of clinical conditions, it will take a prohibitively long time to fracture a tooth in a laboratory setting (Venturini *et al.* 2019). Hence, the step-stress cyclic loading method is often used in dental research for mechanical fatigue testing to reduce test duration (Coelho *et al.* 2009, Silva *et al.* 2011, Borba *et al.* 2013, Venturini *et al.* 2019). With this method, cyclic fatigue is carried out at specified loads with increasing amplitudes, each for a specified time, until the test specimen fails (Nelson 1980). The method has been used extensively for testing the fatigue behaviour of dental materials (Borba *et al.* 2013, Venturini *et al.* 2019) and dental restorations (Coelho *et al.* 2009, Magne *et al.* 2010, Silva *et al.* 2011, 2012). However, it has not been used to test root filled teeth.

Therefore, using the step-stress method, this methodological study aimed to reproduce cracked teeth in a laboratory setting with the aim of producing a more reliable methodology for studying the onset and development of longitudinal cracks in cracked teeth that are currently not well understood.

Materials and methods

The study protocol (no. STUDY00010231) was approved by the Institutional Review Board of the University of Minnesota. Twenty freshly extracted mandibular premolars with a single canal, fully formed apex and similar dimensions were collected. The maximum buccopalatal, mesiodistal widths of the crown and the root length were measured for each sample. The corresponding dimensions were 7.9 ± 0.5, 6.9 ± 0.5 and 13.8 ± 1.1 mm. Each tooth was scanned using micro-computed tomography (micro-CT, HMX-XT 225; Nikon, Brighton, MI, USA) to exclude samples with multiple canals, cracks, caries or previous restorations. The main scanning parameters were as follows: 20-μm isotropic resolution, 115-kV accelerating voltage and 90-μA beam current. The angle of root canal curvature of each sample was measured by Schneider's method (Schneider 1971). All selected samples had relatively straight canals (< 20°).

The sample size was determined using *a priori* power calculation with software G*Power (Heinrich-Heine-Universitat, Dusseldorf, Germany). A pilot study on three samples for each group was performed to calculate the mean and standard deviation of the fracture load. The minimum sample size per group was determined as 7 with a power of 80% and a Type-I error rate of 5%.

Tooth preparation

A standardized mesial-occlusal-distal (MOD) cavity was prepared in each tooth as described elsewhere (Karzoun *et al.* 2015). Subsequently, standard access cavities were prepared using a high-speed handpiece (Midwest Dental Supply, Des Plaines, IL, USA) with air-water cooling.

Each tooth was root filled and restored with resin composite and a fibre post. The working length was established as 1 mm short from the foramen. The root canals were instrumented using ProTaper Gold files (Dentsply, Charlotte, NC, USA) up to F3 (size 30, .09 taper). Irrigation was performed with 10 mL of 5.25% sodium hypochlorite (NaOCl), and the smear layer was removed using 17% EDTA. The canals were filled with gutta-percha points and AH-Plus sealer (Dentsply Sirona, Tulsa, OK, USA) using lateral compaction. All materials used for the following procedures were manufactured by 3 M (St. Paul, MN, USA). In order to maximize the adaptation of the fibre post to the canal wall, the post space was prepared using a RelyX Fibre Post Drill (size 3) 5 mm from the working length. A size-3 glass fibre post (tip size 0.90 mm) was cemented into the canal using RelyX Ultimate Adhesive Resin Cement. The coronal cavity was restored with Filtek One Bulk Fill Composite and Scotchbond Universal Adhesive.

Mechanical test

The root of each tooth was coated with ~0.2-mm-thick polyvinylsiloxane impression material (Express VPS; 3 M ESPE) and then embedded with acrylic resin (Dentsply Caulk, Milford, DE, USA) in a Teflon ring up to 2 mm apical to the CEJ. Loading was conducted at room temperature using a universal testing machine (MTS 858 MiniBionix; II, Eden Prairie, MN, USA) with a 2-mm-diameter stainless-steel hemisphere. During loading, the specimen was kept hydrated by covering it with wet gauze. Distilled water was added to the gauze by using a dropper every 10 mins to keep it hydrated. The 20 prepared specimens were randomly divided into two groups of 10: group 1 was subjected to static loading whilst group 2 was subjected to step-stress cyclic loading.

Group-1 static loading

A static load was applied axially to the centre of the occlusal surface at a crosshead speed of 0.5 mm/min. Fracture was determined from a sharp drop in load, and the peak loads were taken to be the fracture loads.

Group-2 cyclic loading

The loading cycles were sinusoidal at 1 Hz. The minimum load for each cycle was zero whilst the maximum load increased with time. Specifically, the 'step-stress' method (Borba *et al.* 2013) was used, starting with an amplitude of 100 N, followed by 200 and 300 N, each with 1000 cycles (Table 1). Then, the amplitude increased to 400 N, followed by increments of 50 N (i.e. 450 N, 500 N, 550 N...) until 850 N, with 3000 cycles each. If a specimen survived these cycles, loading continued at 850 N until fracture. Fracture was determined from a sudden increase in stroke. The numbers of cycles to failure and the final fracture loads were recorded.

Identification of fracture mode

After loading, each sample was scanned using micro-CT again to identify the fracture mode. There were three modes: 1. longitudinal fracture, where an incomplete crack initiated from the crown and propagated longitudinally to 'subgingival' dentine; 2. cuspal fracture, where a complete or incomplete fracture initiated from the crown and propagated subgingivally, leading to a fractured cusp; 3. mixed-mode fracture, that is a combination of longitudinal and cuspal fracture.

Statistical analysis

Statistical analysis was performed using SPSS (SPSS Inc., Chicago, IL, USA). Parametric distribution and

Table 1 Loading amplitudes and corresponding numbers of cycles for accelerated fatigue test

Loading amplitude (N)	Number of cycles
100	1000
200	1000
300	1000
400	3000
450	3000
500	3000
550	3000
600	3000
650	3000
700	3000
750	3000
800	3000
850	Until fracture

homogeneity of variances were verified. Differences in fracture load between the groups were analysed using Student's *t*-test. The level of significance was set at 0.05. Further, the samples in each group were ranked in an ascending order according to their fracture loads. The failure probability (P_f) of each sample was then calculated using the following estimator (Bergman 1984, Quinn & Quinn 2010):

$$P_f = \frac{i}{n+1},$$

where *i* is the rank of the specimen within a group of size *n*.

Results

Fracture load and average load per cycle

The mean fracture loads for the static loading and cyclic loading groups were 769 ± 171 N and 720 ± 92 N, respectively. There was no significant difference between the two groups ($P > 0.05$).

In the cyclic loading group, longitudinal fractures occurred with a larger number of cycles to failure and a higher average load per cycle, whilst cuspal fractures occurred with a smaller number of cycles and a lower average load per cycle (Fig. 3a). For the longitudinal, cuspal and mixed-mode fractures, respectively, the average loads per cycle were 561 ± 70 N, 429 ± 56 N and 466 ± 87 N. The respective numbers of cycles to failure were 32297 ± 12624, 17640 ± 7760 and 20202 ± 9829. Note that, due to the increasing load amplitude of the fatigue test, as the number of cycles to failure increased, both the fracture load and the average load per cycle also increased (Fig. 3a). Dentinal failures were more likely to happen in samples that failed with higher loads, irrespective of the mode of loading.

Fracture modes

The proportions of longitudinal, cuspal and mixed-mode fractures in the cyclic loading group were 50, 20 and 30%, respectively (Fig. 1). In the static loading group, only cuspal fractures occurred (Fig. 2).

In all the five teeth with longitudinal fracture, the position and orientation of the cracks were relatively consistent. From the transverse cross sections, it can be seen that the fracture oriented mesiodistally, dividing the root section into two approximately equal halves (Fig. 1a). From the sagittal view, a clear fracture line can be seen starting from the composite restoration and longitudinally propagating into the root. However, the fracture was arrested and did not completely split the tooth (Fig. 1b). No other cracks were obvious in dentine.

In the teeth with cuspal fractures, a main crack started from the occlusal surface and propagated obliquely to the CEJ (Fig. 1d). Small cracks randomly oriented around the main crack could also be observed (Fig. 1c). In mixed-mode fracture, the crack began from the occlusal surface and propagated longitudinally up to the middle third of the root, where it turned obliquely and finally caused catastrophic fracture (Fig. 1f).

The cuspal fractures in the static loading group (Fig. 2) were similar to those in the cyclic loading group. Most of them started from the occlusal surface close to the loading area and propagated obliquely, involving both dentine and resin composite. They finally reached the CEJ and led to the fracture of a cusp.

Failure probability

Figure 3b shows the increase in failure probability with increasing load for both groups. Between the two groups, the cyclic loading group had a lower fracture load for the same failure probability. The failure probability against average load per cycle for the cyclic loading group is shown in Fig. 3c. The trend is similar to that for the fracture load (Fig. 3b). Again, samples with cuspal fractures tended to have a lower average load per cycle, whilst samples with longitudinal fractures tended to have a higher average load per cycle.

Discussion

Several factors can influence the load capacity of root filled teeth. First, excessive tooth tissue loss during root canal treatment could reduce its load capacity (Kishen 2006). However, whether root canal treatment could induce dentinal micro-cracks is still under debate (PradeepKumar *et al.* 2019, Zaslansky *et al.* 2020). Another factor is the loss of water-rich pulp tissues and, hence, free water from dentine (Huang *et al.* 1992), which may adversely affect their biomechanical behaviour (Kishen 2006). It has been reported that dentine from root canal-restored teeth exhibited more extensive collagen cross-linking and less dentinal tubule occlusion than that in unrestored
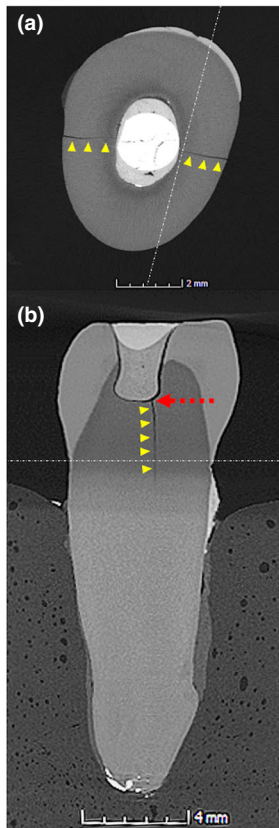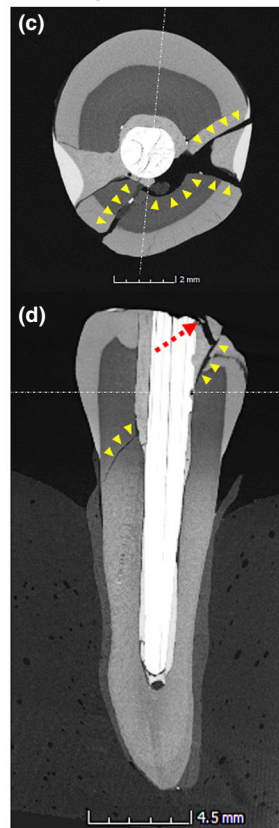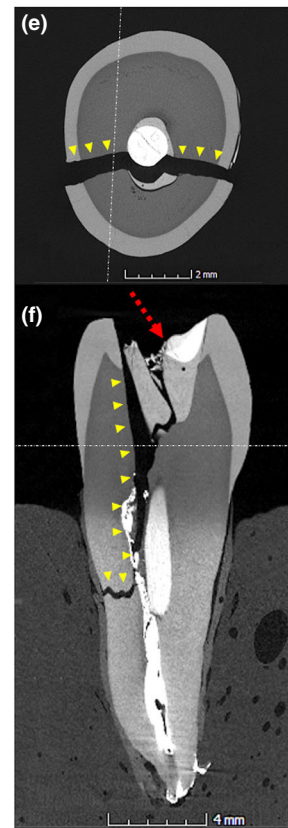
Figure 1 Micro-CT images showing different fractures modes in the cyclic loading group: (a, b) longitudinal fracture, (c, d) cuspal fracture and (e, f) mixed-mode fracture. The yellow triangles indicate the positions of the main failure. The red dashed arrows indicate the possible positions of crack initiation. The white dashed line in each section indicates the position of the other corresponding section of the same fracture mode.

teeth (Yan *et al.* 2019). The age of the tooth is also an influencing factor as the fracture resistance of dentine changes with age (Yan *et al.* 2020).

MOD cavities were prepared in this study to weaken the samples so as to limit the number of cycles to failure (Ratcliff *et al.* 2001). Also, single-rooted premolars were tested to avoid the large variations in fracture progression caused by the varied root and root canal configurations in multi-rooted teeth (Krishnan *et al.* 2018).

Cyclic loading was used to induce longitudinal cracks as mechanical fatigue is considered a critical factor in the occurrence of cracked teeth (Banerji *et al.* 2010). To mimic oral mastication, the study adopted sinusoidal load cycles with a zero minimum load. The frequency of loading was 1 Hz, in accordance with that of intraoral chewing (Kruzic *et al.* 2005). In particular, fatigue was accelerated with the

step-stress approach (Borba *et al.* 2013): starting from a load amplitude of 100 N and successively increasing it to 850 N. This was also used to limit the total testing time to an acceptable duration; it would be impractical to use a clinically relevant but low load because of the prohibitively long time to failure (Venturini *et al.* 2019). The step-stress method has never been used for producing stable longitudinal cracks in root filled teeth. Regarding the increasing load levels, the first and the last load amplitudes were set at 10% and 100%, respectively, of the mean failure load for the first three samples tested statically, as described elsewhere (Borba *et al.* 2013).

Micro-CT was used to identify the internal cracks and fracture modes of the specimens nondestructively (Orhan *et al.* 2018). In most previous studies, the fracture patterns were merely observed by the naked eye or using an optical microscope (Karzoun *et al.*
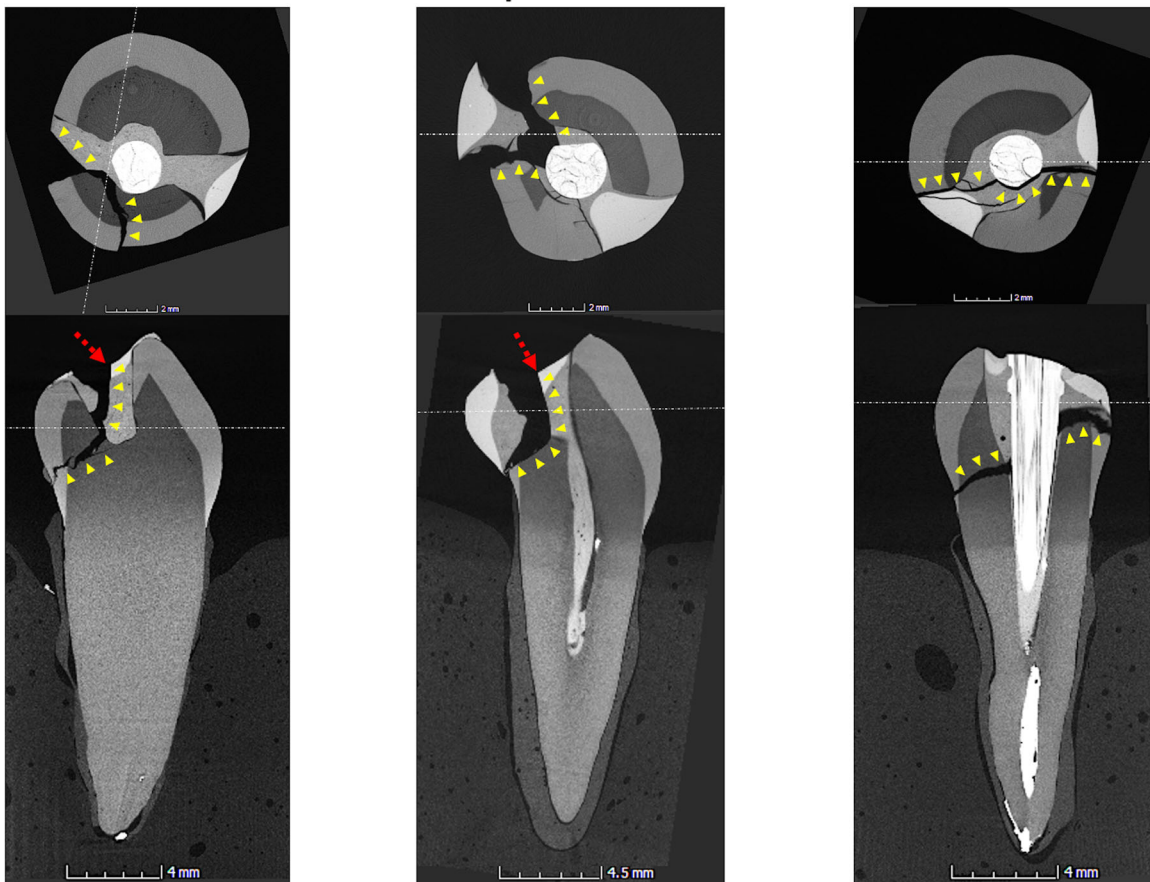
Cuspal fracture

Figure 2 Micro-CT images showing representative cuspal fractures in the static loading group. The yellow triangles indicate the positions of the main failure. The red dashed arrows indicate the possible positions of crack initiation. The white dashed line in each section indicates the position of the other corresponding section of the same fracture mode.

2015, Xiong *et al.* 2015). This way, cracks that occurred inside the tooth or subgingivally cannot be seen easily. As a result, the fracture patterns were simply described as 'restorable/favourable' or 'unrestorable/unfavourable' (Uzun *et al.* 2015, Plotino *et al.* 2017, Özyürek *et al.* 2018) without the detailed descriptions given in this study.

Stable longitudinal cracks were produced in the cyclic loading group only, whereas unstable cuspal fractures happened in all the samples in the static loading group. Other studies that used a static load also produced cuspal fractures rather than a longitudinally cracked tooth (Franco *et al.* 2014, Karzoun *et al.* 2015, Plotino *et al.* 2017, Özyürek *et al.* 2018), as shown in the present study. This is attributed to the difference in the level of stored strain energy

between the two groups at crack initiation (Kruzic *et al.* 2005). Static loading allowed strain energy to be built up to a level sufficient for unstable crack propagation prior to crack initiation (Hayashi *et al.* 2008). Cyclic loading, on the other hand, caused early crack initiation through fatigue at a relatively low load and strain energy level. Thus, the crack was able to propagate slowly during cyclic fatigue (Arola 2017).

The position of crack initiation appeared to be different between the two loading modes. The longitudinal cracks in the cyclic loading group appeared to start below the resin composite, whereas the cuspal fractures observed in both groups appeared to start from the area near the loading point. Indeed, fracture of restored teeth caused by static loading normally
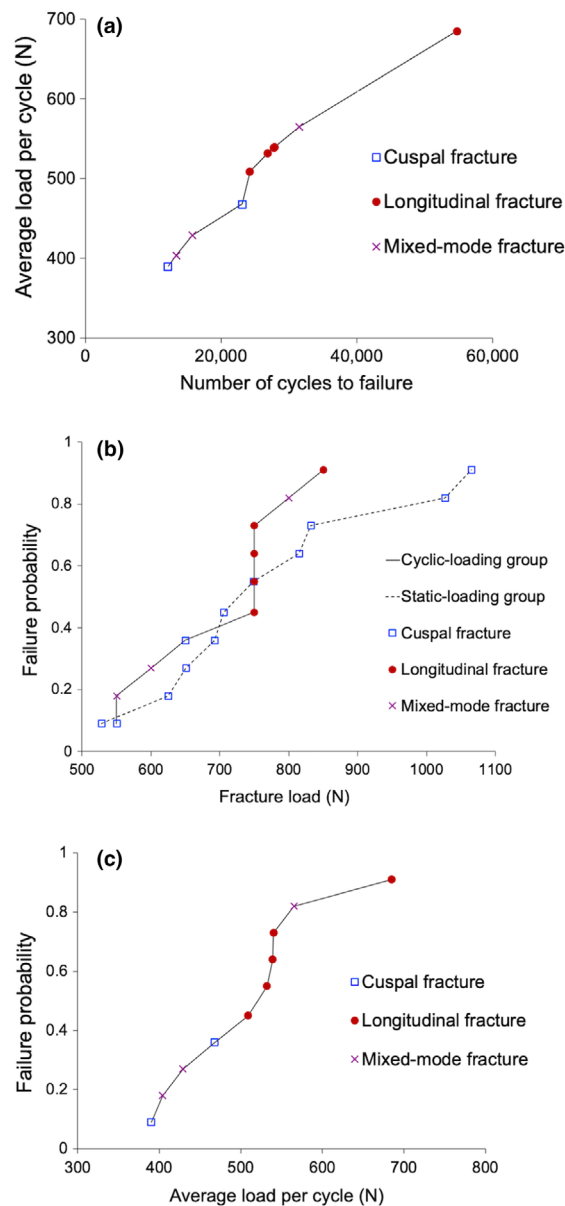
Figure 3 (a) Average load per cycle against number of cycles to failure for the cyclic loading group. (b) Failure probability against fracture load for both groups. (c) Failure probability against average load per cycle for the cyclic loading group.

initiates from the locations of stress concentration near the loading point (Hayashi *et al.* 2008, Plotino *et al.* 2017, Özyürek *et al.* 2018). However, an analysis of crack initiation or propagation is usually absent in these studies. Fracture would occur when the local stresses exceed the fracture strength of the materials.

The main difference between static and fatigue failure is that in fatigue failure, the intrinsic strength of the materials reduces with the number of load cycles (Yahyazadehfar *et al.* 2013). As far as dental materials are concerned, the dentine-composite interface is more vulnerable to fatigue compared with its constituents, dentine and composite, due to its lower fatigue strength (Zhang *et al.* 2015). Moreover, cyclic loading could change the viscoelastic property of the interface which helps to dissipate stresses (Toledano *et al.* 2017, 2018). As a result, interfacial failure may occur prior to tooth fracture, which leads to the development of stress concentrations at the internal line angles of the cavity. Further studies such as finite element and interfacial fatigue analysis should be performed to confirm whether interfacial debonding and stress redistribution did happen during the fatigue test to better understand the mechanisms for structural failures in endodontically treated teeth.

In this study, the longitudinal cracks produced in the cyclic loading group extended mesiodistally and apically, which are similar to those found clinically (Rivera & Walton, 2008) and more consistent than those reported in other studies. These other studies commonly used a thermal shock to induce cracking (Wang *et al.* 2017, Yuan *et al.* 2020). However, the orientation of the crack was hard to control and most teeth ended up with multiple cracks in different directions and positions (Yuan *et al.* 2020). In the present study, longitudinal cracks similar to those found clinically were produced in 50% of the samples in the cyclic loading group. The lack of such longitudinal cracks in the static loading group is an important observation that future studies addressing the load capacity of root filled teeth will need to explore. Further studies using finite element and stress-life analyses should be performed to study numerically the initiation and propagation of the longitudinal crack in endodontically treated teeth in more detail. It would be also instructive to repeat some studies on minimally invasive access using fatigue loading (Plotino *et al.* 2017, Corsentino *et al.* 2018).

Conclusion

Longitudinally cracked teeth have been successfully produced in a laboratory setting using a step-stress cyclic loading method. This provides a more clinically representative yet practical methodology for studying the aetiology, propagation, influencing factors, detection and treatments of cracked teeth.

Acknowledgement

Conflict of interest

The authors have stated explicitly that there are no conflicts of interest in connection with this article.

References

Alkhalifah S, Alkandari H, Sharma PN, Moule AJ (2017) Treatment of cracked teeth. *Journal of Endodontics* **43**, 1579–86.

Arola D (2017) Fatigue testing of biomaterials and their interfaces. *Dental Materials* **33**, 367–81.

Banerji S, Mehta SB, Millar BJ (2010) Cracked tooth syndrome. Part 1: aetiology and diagnosis. *British Dental Journal* **208**, 459–63.

Bergman B (1984) On the estimation of the Weibull modulus. *Journal of Materials Science Letters* **3**, 689–92.

Berman LH, Kuttler S (2010) Fracture necrosis: diagnosis, prognosis assessment, and treatment recommendations. *Journal of Endodontics* **36**, 442–6.

Borba M, Cesar PF, Griggs JA, Della Bona Á (2013) Step-stress analysis for predicting dental ceramic reliability. *Dental Materials* **29**, 913–8.

Coelho PG, Bonfante EA, Silva NRF, Rekow ED, Thompson VP (2009) Laboratory simulation of Y-TZP all-ceramic crown clinical failures. *Journal of Dental Research* **88**, 382–6.

Corsentino G, Pedullà E, Castelli L *et al.* (2018) Influence of access cavity preparation and remaining tooth substance on fracture strength of endodontically treated teeth. *Journal of Endodontics* **44**, 141621.

Franco ÉB, Lins do Valle A, Pompéia Fraga de Almeida AL, Rubo JH, Pereira JR (2014) Fracture resistance of endodontically treated teeth restored with glass fiber posts of different lengths. *Journal of Prosthetic Dentistry* **111**, 30–4.

Hayashi M, Sugeta A, Takahashi Y, Imazato S, Ebisu S (2008) Static and fatigue fracture resistances of pulpless teeth restored with post-cores. *Dental Materials* **24**, 1178–86.

Huang TJG, Schilder H, Nathanson D (1992) Effects of moisture content and endodontic treatment on some mechanical properties of human dentin. *Journal of Endodontics* **18**, 209–15.

Kang SH, Kim BS, Kim Y (2016) Cracked teeth: distribution, characteristics, and survival after root canal treatment. *Journal of Endodontics* **42**, 557–62.

Karzoun W, Abdulkarim A, Samran A, Kern M (2015) Fracture strength of endodontically treated maxillary premolars supported by a horizontal glass fiber post: an in vitro study. *Journal of Endodontics* **41**, 907–12.

Kelly JR (1997) Ceramics in restorative and prosthetic dentistry. *Annual Review of Materials Science* **27**, 443–68.

Kishen A (2006) Mechanisms and risk factors for fracture predilection in endodontically treated teeth. *Endodontic Topics* **13**, 57–83.

Krishan R, Paqué F, Ossareh A, Kishen A, Dao T, Friedman S (2014) Impacts of conservative endodontic cavity on root canal instrumentation efficacy and resistance to fracture assessed in incisors, premolars, and molars. *Journal of Endodontics* **40**, 1160–6.

Krishnan U, Moule A, Michael S, Swain M (2018) Fractographic analysis of a split tooth presenting radiographically as a horizontal root fracture in an unrestored mandibular second molar. *Journal of Endodontics* **44**, 304–11.

Kruzic JJ, Nalla RK, Kinney JH, Ritchie RO (2005) Mechanistic aspects of in vitro fatigue-crack growth in dentin. *Biomaterials* **26**, 1195–204.

Li Y, Carrera C, Chen R *et al.* (2015) Fatigue failure of dentin-composite disks subjected to cyclic diametral compression. *Dental Materials* **31**, 778–88.

Magne P, Schlichting LH, Maia HP, Baratieri LN (2010) In vitro fatigue resistance of CAD/CAM composite resin and ceramic posterior occlusal veneers. *Journal of Prosthetic Dentistry* **104**, 149–57.

Nelson W (1980) Accelerated life testing - step-stress models and data analyses. *IEEE Transactions on Reliability* **R-29**, 103–8.

Nishigawa K, Bando E, Nakano M (2001) Quantitative study of bite force during sleep associated bruxism. *Journal of Oral Rehabilitation* **28**, 485–91.

Orhan K, Jacobs R, Celikten B *et al.* (2018) Evaluation of threshold values for root canal filling voids in micro-CT and nano-CT images. *Scanning* **2018**, 9437569.

Özyürek T, Ülker Ö, Demiryürek EÖ, Yılmaz F (2018) The effects of endodontic access cavity preparation design on the fracture strength of endodontically treated teeth: traditional versus conservative preparation. *Journal of Endodontics* **44**, 800–5.

Plotino G, Grande NM, Isufi A *et al.* (2017) Fracture strength of endodontically treated teeth with different access cavity designs. *Journal of Endodontics* **43**, 995–1000.

PradeepKumar AR, Shemesh H, Archana D *et al.* (2019) Root canal preparation does not induce dentinal microcracks in vivo. *Journal of Endodontics* **45**, 1258–64.

Quinn JB, Quinn GD (2010) A practical and systematic review of Weibull statistics for reporting strengths of dental materials. *Dental Materials* **26**, 135–47.

Ratcliff S, Becker IM, Quinn L (2001) Type and incidence of cracks in posterior teeth. *Journal of Prosthetic Dentistry* **86**, 168–72.

Rivera E, Walton ER (2008) *Cracking the cracked tooth code: detection and treatment of various longitudinal tooth fractures.* Endodontics: Colleagues for Excellence Summer, 2–7.

Rivera EM, Walton RE (2007) Longitudinal tooth fractures: findings that contribute to complex endodontic diagnoses. *Endodontic Topics* **16**, 82–111.

Sapra A, Darbar A, George R (2020) Laser-assisted diagnosis of symptomatic cracks in teeth with cracked tooth: a 4-year in-vivo follow-up study. *Australian Endodontic Journal* **46**, 197–203.

Schneider SW (1971) A comparison of canal preparations in straight and curved root canals. *Oral Surgery, Oral Medicine, Oral Pathology* **32**, 271–5.

Seo DG, Yi YA, Shin SJ, Park JW (2012) Analysis of factors associated with cracked teeth. *Journal of Endodontics* **38**, 288–92.

Silva NRFA, Bonfante EA, Rafferty BT *et al.* (2011) Modified Y-TZP core design improves all-ceramic crown reliability. *Journal of Dental Research* **90**, 104–8.

Silva NRFA, Bonfante E, Rafferty BT *et al.* (2012) Conventional and modified veneered zirconia vs. metalloceramic: fatigue and finite element analysis. *Journal of Prosthodontics* **21**, 433–9.

Sim IGB, Lim TS, Krishnaswamy G, Chen NN (2016) Decision making for retention of endodontically treated posterior cracked teeth: a 5-year follow-up study. *Journal of Endodontics* **42**, 225–9.

Tan L, Chen NN, Poon CY, Wong HB (2006) Survival of root filled cracked teeth in a tertiary institution. *International Endodontic Journal* **39**, 886–9.

Toledano M, Osorio R, López-López MT *et al.* (2017) Mechanical loading influences the viscoelastic performance of the resin-carious dentin complex. *Biointerphases* **12**, 021001.

Toledano M, Osorio R, Osorio E, Cabello I, Toledano-Osorio M, Aguilera FS (2018) In vitro mechanical stimulation facilitates stress dissipation and sealing ability at the conventional glass ionomer cement-dentin interface. *Journal of Dentistry* **73**, 61–9.

Uzun I, Arslan H, Doǧanay E, Güler B, Keskin C, Çapar ID (2015) Fracture resistance of endodontically treated roots with oval canals restored with oval and circular posts. *Journal of Endodontics* **41**, 539–43.

Venturini AB, Prochnow C, Pereira GKR, Segala RD, Kleverlaan CJ, Valandro LF (2019) Fatigue performance of adhesively cemented glass-, hybrid- and resin-ceramic materials for CAD/CAM monolithic restorations. *Dental Materials* **35**, 534–42.

Wang S, Xu Y, Shen Z *et al.* (2017) The extent of the crack on artificial simulation models with CBCT and periapical radiography. *PLoS One* **12**, 1–12.

Wu S, Lew HP, Chen NN (2019) Incidence of pulpal complications after diagnosis of vital cracked teeth. *Journal of Endodontics* **45**, 521–5.

Xiong Y, Huang SH, Shinno Y *et al.* (2015) The use of a fiber sleeve to improve fracture strength of pulpless teeth with flared root canals. *Dental Materials* **31**, 1427–34.

Yahyazadehfar M, Mutluay MM, Majd H, Ryou H, Arola D (2013) Fatigue of the resin-enamel bonded interface and the mechanisms of failure. *Journal of the Mechanical Behavior of Biomedical Materials* **21**, 121–32.

Yan W, Chen H, Fernandez-Arteaga J, Paranjpe A, Zhang H, Arola D (2020) Root fractures in seniors: Consequences of acute embrittlement of dentin. *Dental Materials* **36**, 1464–73.

Yan W, Montoya C, Øilo M *et al.* (2019) Contribution of root canal treatment to the fracture resistance of dentin. *Journal of Endodontics* **45**, 189–93.

Yuan M, Gao AT, Wang TM *et al.* (2020) Using meglumine diatrizoate to improve the accuracy of diagnosis of cracked teeth on cone-beam CT images. *International Endodontic Journal* **53**, 709–14.

Zaslansky P, Prates Soares A, Shemesh H (2020) Root dentinal microcracks - absence of evidence is not evidence of absence. *International Endodontic Journal* **53**, 135–6.

Zhang Z, Beitzel D, Mutluay M, Tay FR, Pashley DH, Arola D (2015) On the durability of resin-dentin bonds: Identifying the weakest links. *Dental Materials* **31**, 1109–18.